Renewable Energy 207 (2023) 731–742

Contents lists available at ScienceDirect

Renewable Energy

journal homepage: www.elsevier.com/locate/renene

Development of a reliable simulation framework for techno-economic analyses on green hydrogen production from wind farms using alkaline electrolyzers

Francesco Superchi [a], Francesco Papi [a], Andrea Mannelli [a], Francesco Balduzzi [a], Francesco Maria Ferro [b], Alessandro Bianchini [a,*]

[a] Department of Industrial Engineering, Università degli Studi di Firenze, Florence, Italy
[b] McPhy Energy Italia, Via Ayrton Senna 22, 56028, San Miniato, PI, Italy

ARTICLE INFO

Keywords:
Green hydrogen
Electrolysis
Batteries
Hybrid energy storage systems
Wind turbine
Levelized cost of hydrogen

ABSTRACT

The present study investigates the feasibility of coupling the intermittent electric power generation from a wind farm with alkaline electrolyzers to produce green hydrogen. A physically accurate model of commercial electrolytic modules has been first developed, accounting for conversion efficiency drop due to modules' cool down, effects of shutdowns due to the intermittence of wind power, and voltage degradation over the working time frame. The model has been calibrated on real modules, for which industrial data were available. Three commercial module sizes have been considered, i.e., 1, 2 and 4 MW. As a second step, the model has been coupled with historical power datasets coming from a real wind farm, characterized by a nominal installed power of 13.8 MW. Finally, the model was implemented within a sizing algorithm to find the best combination between the actual wind farm power output and the electrolyzer capacity to reach the lowest Levelized Cost Of Hydrogen (LCOH) possible. To this end, realistic data for the capital cost of the whole system (wind farm and electrolyzers) have been considered, based on industrial data and market reports, as well as maintenance costs including both periodic replacements of degraded components and periodic maintenance. Simulations showed that, if the right sizing of the two systems is made, competitive hydrogen production costs can be achieved even with current technologies. Bigger modules are less flexible but, by now, considerably cheaper than smaller ones. A future economy of scale in alkaline electrolyzers is then needed to foster the diffusion of the technology.

1. Introduction

It is well known that hydrogen does not exist in its pure state on Earth and must be obtained currently by means of energy demanding processes, starting from fossil fuels or renewable sources. In this view, low-carbon hydrogen is gaining increasing attention for the decarbonization of the energy sector. Depending on the production process and primary power source, hydrogen is often classified by colors. Currently, the largest amount of produced hydrogen is "grey", i.e., obtained starting from fossil fuels by means of steam reforming of methane or gasification of coal. Greenhouse gases (GHG) are released during grey hydrogen production processes. If a carbon capture system (CCS) is applied to these processes to reduce GHG emissions, the hydrogen produced can be classified as "blue". Alternatively, hydrogen can be produced from water by electrolysis: water splitting in oxygen and hydrogen by means of an electric current. If this electrochemical process is powered by electricity coming from renewable sources, hydrogen can be classified as "green" [1].

In the context of the energy transition towards the decarbonization of our society, hydrogen is among the most promising energy storage technologies. Wind, solar and other renewable energy sources (RES) will play a significant role in the decarbonization of the energy sector. The main drawback of those technologies is their intermittent production, caused by the inherent fluctuating nature of solar radiation and wind. By means of a power-to-gas process [2], green hydrogen can be produced by water electrolysis for the purpose of being reconverted in electric power in a subsequent moment.

Hydrogen may also increase the flexibility of renewable generators and allow the full exploitation of windy, yet remote locations that show a high-RES power potential. Coastal areas are, for example, characterized by higher wind speeds [3], but the often weak connection to the

* Corresponding author.
E-mail address: alessandro.bianchini@unifi.it (A. Bianchini).

https://doi.org/10.1016/j.renene.2023.03.077
Received 16 December 2022; Received in revised form 9 March 2023; Accepted 16 March 2023
Available online 17 March 2023

Nomenclature

C	cost
c	specific heat, J/kgK
CAPEX	capital expenditures
CCS	carbon capture system
CF	capacity factor
D	degradation
EFC	equivalent number of full charge-discharge cycles
GHG	greenhouse gases
h	convection coefficient, W/m2K
H	hydrogen
i	current density, A
I	current, A
k	conduction coefficient, W/mK
L	length, m
LCOH	levelized cost of hydrogen, €/kg
m	mass, kg
n	number
OPEX	operational expenditures
P	power
PV	photovoltaics
q	thermal power, W
Q	thermal energy, Wh
r	discount rate
R	radius, m
RES	renewable energy sources
SCADA	supervisory control and data acquisition
SOC	state of charge
SOH	state of health
T	Temperature, °C
V	voltage, V
WT	wind turbine
x	size

Greek symbols

α	scale factor
η	efficiency
φ	conversion factor, kg/kWh

Subscripts and superscripts

a	air
c	charge
d	discharge
e	external
el	electrolyzer
es	electrolytic solution
gw	glass wool
i	internal
id	ideal
m	module
op	operational
PV	photovoltaics
t	tank
tn	thermoneutral
WT	wind turbine

electricity grid may hamper installation of generators in such locations. The same applies to offshore wind turbine technology [4], whose positioning may often be close to remote land areas. Green hydrogen, as other storage means, can be useful to exploit power curtailments and transport energy produced by those plants in an alternative way [5]. Lin et al. [6] proved that a cost-competitive green hydrogen may contribute to significantly reducing wind curtailments and CO_2 emissions.

Green hydrogen and sustainable fuels derived from it (ammonia, methanol or aviation fuels) can play a crucial role in the decarbonization of the hard-to-abate sectors. It has the potential to become a low-carbon fuel for heavy-duty transportations as trucks and container ships. This potential could be further increased with the development of a hydrogen infrastructure [7]. Another interesting application could be in heavy industries, where hydrogen can provide low carbon heat for metallurgic process as steel production or reducing gas for processes in chemical industries [8]. In Ref. [9], some of the authors have investigated the potential for green hydrogen production capability of a grid-connected wind farm for the steal manufacturing decarbonization.

The main issue hampering wider diffusion of green hydrogen is its current cost. To gain market potential, it must in fact become competitive with respect to grey hydrogen. Currently, grey hydrogen has a levelized cost of 1–1.4 €/kg, while green hydrogen produced, for example, via wind-powered water electrolysis, has a cost of 3.75–5.11 €/kg [10]. However, research and development actions are being put in place, with hydrogen roadmaps released by more than 30 countries worldwide and more than 70 billion $ of public funds granted to hydrogen projects in 2020 (McKinsey, pers. comm., 2021). As part of an ongoing research program on alkaline electrolysis at large scale, the aim of the present study is to develop a reliable simulation framework for techno-economic analyses on green hydrogen production from renewable energy sources.

1.1. State of the art in green hyrogen production

Surveys about the potential for green hydrogen production from various sites or plant configurations have been receiving significant attention in scientific literature. Mazzeo et al. [11] studied the integration of different renewable generators, wind and solar, for the large-scale production of hydrogen. The authors developed a methodology to compare renewable based systems in different sites around the globe.

Bhandari et al. [12] performed a techno-economic assessment of decentralized hydrogen production in Europe. In that study they compared six scenarios, considering the national grid support, an auxiliary battery support, and two different electrolyzers technologies (alkaline and PEM). They found that grid connected solar photovoltaic systems that powered an alkaline electrolyzers led to optimal results in economic terms (6.23 €/kg), proving the potential of this technology among the others.

Nastasi et al. [13] considered off-grid configurations in which green hydrogen is produced in isolated systems as storage mean (power-to-gas). They compared this solution with batteries and found that a further reduction in the LCOH is necessary to make power-to-gas competitive in the market. Accurate performance projections and analysis are key to understanding the cost reduction perspective of green hydrogen technologies.

1.2. Aims of the study and novelty

This study proposes a parametric model developed to assess the hydrogen production capabilities of an off-grid hybrid system that powers alkaline electrolyzers with electricity produced by a wind farm (Fig. 1); the most suitable sizing has been analyzed as a function of the number and size of installed electrolyzer modules and of the capacity of an energy storage system.

The original model of the electrolyzer has been developed in Python

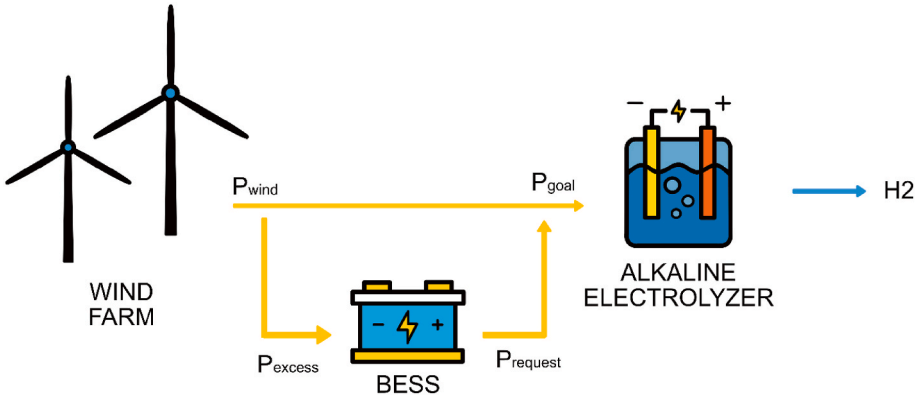

Fig. 1. Off-grid wind powered water electrolysis with BESS support.

for the purpose of this analysis and has been calibrated on actual data of a commercial device produced by McPhy Energy, a leading alkaline electrolyzer company.

This work may contribute to the literature in many regards. First, the collaboration with an established alkaline electrolyzer manufacturer allowed the creation of a model that considers all the key aspect of the intermittent hydrogen production while keeping the framework light in computational costs. Second, real production history of an actual wind farm was utilized as input to test the estimation capabilities of the developed simulation framework, as step forward with respect to studies that consider synthetic data.

Several alkaline electrolyzers models have been described in literature. Genovese et al. [14] developed an accurate zero-dimensional model able to follow a multi-physics and dynamic approach. A description of all the main phenomena occurring into the device is compelling, but it carries high computational costs. Differently, the aim of this work was to develop a simple yet effective model able to simulate a high number of hydrogen production plant configurations on extended time periods to assess long-term performance and optimize components' size.

The collaboration with a manufacturing company allowed focusing on the most influential factors to correctly estimate the hydrogen production capability of this specific system. In particular, the possibility to perform parametric analyses with a limited computational cost enables the production of techno-economic performance maps that can help the designing phase of new plants.

Most of the techno-economic studies in literature strongly simplify the electrolyzer behavior. Rezaei et al. [15] analyzed different cases related to wind energy use for hydrogen production in underdeveloped countries. The economic investigation was based on a hydrogen productivity assessment with a constant power-to-gas conversion factor. Since this approach considers the variation of the power-to-gas conversion factor, the model proposed herein may represent a step forward for studies on the theme.

Another example is represented by studies that aim to assess the potential of the hydrogen vector for seasonal storage, as the one done by Marino et al. [16]. Chade et al. [17] performed a work using similar tools to assess the feasibility of a wind-to-hydrogen system for artic remote locations. A lightweight electrolyzer model, able to capture the most important variations about the cell performance, may bridge the gap between initial estimations and the actual performance of the electrolyzer.

The study is organized as follows. Section 2 presents the datasets available for the study and the numerical methods developed herein. The results of the parametric analyses are reported in Section 3, in terms of system producibility and Levelized Cost Of Hydrogen (LCOH). Section 4 finally draws some conclusions and proposes future research actions to further improve the competitiveness of wind-powered green hydrogen production.

2. Methods

This section explains in detail the main inputs for the analysis and how they are combined to reach the targets of the analysis. First, the wind power production dataset is presented and described. Then, a description if provided on how the behavior of the main components of the system is modelled and characterized in Python.

2.1. Wind data

Unlike most of existing studies, where wind series are hypothesized or derived from short-time measured data (e.g., Refs. [18–20]), the present study benefits from actual power production data of a utility-scale wind farm located in Greece.

The pairing between electrolysis and wind energy was also considered by Razzaqul et al. [21], who analyzed the prospect of the wind-to-hydrogen technology deriving the power production capabilities of wind energy using the power curve of a commercial generator. The current study takes into account real production data from an actual wind farm, thereby reducing bias in the results. The farm is composed by six onshore wind turbines (WTs), each of which is characterized by a nominal output power of 2.3 MW.

Wind and power data coming from the Supervisory Control and Data Acquisition (SCADA) system was kindly provided by Eunice Energy Group (EEG) with a time resolution of 10 min. The original dataset was analyzed and cleaned: errors or abnormal values related to periods of maintenance, lightning and icing were removed. The produced power history of one year of operation is given as input to the model.

2.2. Alkaline electrolyzer

Among the water splitting technologies, alkaline water electrolysis (ALK) is the most mature and commercially diffused, with a market share of about 70% [22]. This technology benefits from low cost and long operational life, and it is characterized by an electrical efficiency up to 70% [1].

Electrolyzer stacks are composed by a series connection of multiple electrolytic cells. In this kind of system, each cell is built by a pair of electrodes immersed in an electrolyte and separated by a diaphragm [23].

The electrolyte used in alkaline water electrolyzers is an alkaline solution of water and potassium hydroxide (KOH) at concentration of 25–30% wt. because of the optimal conductivity and remarkable corrosion resistance of stainless steel in this concentration range [24]. In each cell, the water electrolysis process takes place: water is split into hydrogen and oxygen by means of an electric power applied to the two

electrodes. Electric power is absorbed by the electrolyzer to maintain a certain voltage and current density to activate the conversion reaction.

Voltage and current of a cell are linked by a polarization curve (f_{i-v}) that accounts for irreversible processes. The real operating voltage is given by the sum of the minimum theoretical voltage required by the water splitting reaction and three overpotentials caused by activation, ohmic and concentration losses [25].

2.2.1. Electrolyzer model

In order to limit the computational costs of the electrolyzer model for the practical reasons explained in Section 1, the linear portion of the polarization curve is only considered, where the device works at intermediate current densities and the cell potential is i.e., affected by the second kind of losses, increasing linearly with current due to ohmic overpotentials.

2.2.2. Polarization curve shift

At rated power, the cell works at the highest point of the curve, which corresponds to a current density of 10 kA/m^2 and a voltage of 1.89 V.

The polarization curve translates towards higher voltages if the temperature decreases (Fig. 2 (a)), meaning that to obtain the same current density the cell must work at a higher voltage when the working temperature is below the rated temperature. Working time has the same effect on the polarization curve. Fig. 2 (b) shows that years of operation lead to a parallel upward shift.

The produced hydrogen flow rate is assumed to be directly proportional to the cell current density and this connection is described by a function f_{H2-i}. With the increase of current density, the cell starts producing hydrogen up to a rated value of 1.9 Nm^3/h.

According to Eq. (1), the current that flows in a cell can be calculated by multiplying the current density i by the cell surface S. A single cell is characterized by a 0.5 m^2 round section.

$$I = i \cdot S = 10 \frac{kA}{m^2} \cdot 0.5\ m^2 = 5\ kA \tag{1}$$

Power absorbed by one cell is given by the multiplication between the previously calculated current and the cell voltage V.

According to Eq. (2), a single cell needs 9.45 kW at rated conditions. This means that a 1 MW module incorporates around 106 cells.

$$P = V \cdot I = 1.89\ V \cdot 5\ kA = 9.45\ kW \tag{2}$$

During operation, the polarization curve changes because of time and temperature. At each timestep, the model employs Eq. (3) to quantify the voltage variation. In actual high current stack technology, time degradation ($\Delta V_{time,deg}$) consists in an increase of 3 μV per working hour while thermal degradation ($\Delta V_{temperature,deg}$) rises the voltage of 5 mV per degree of cool down with respect to rated conditions[1].

$$V_{op} = V_{ideal} + \Delta V_{time,deg} \cdot h_{work} + \Delta V_{Thermal,deg} \cdot (T_{rated} - T_{el}) \tag{3}$$

The operating voltage allows estimating the working conditions of the module: the operating polarization curve (f_{i-v}) and the conversion factor (φ). The latter represents a transfer function between the input power to the module and the hydrogen flow rate that can be produced. At each time step, φ is computed by using the maximum hydrogen production $H_{2,id}$ and the ideal current I_{id}, while the voltage V_{op} is affected by time and thermal degradation (Eq. (4))). This value can then be used to estimate the amount of hydrogen that the module is able to produce, given the available amount of power produced by the wind farm.

$$\varphi = \frac{H_{2,id}}{n_{cells} \cdot V_{op} \cdot I_{id}} \tag{4}$$

Power fed to the electrolyzer stack at each time step is partitioned between the number of modules that can be activated, considering that each module requires at least 20% of its rated power.

Ren et al. [26] performed experimental studies on alkaline electrolyzers and assessed an inferior operational limit, in their case 30% nominal load. This model considers how this limitation affects the producibility of these systems when connected to intermittent power sources. The power partitioning algorithm aims to keep the highest possible number of modules activated, allocating the minimum required power to many modules as possible.

After the power allocation, the hydrogen production per module ($H2_{prod,m}$) is obtained based on the previously estimated φ (Eq. (5)).

$$H2_{prod,m} = \varphi_m \cdot P_{allocated,m} \tag{5}$$

2.2.3. Thermal model of the electrolyzer

Based on the current hydrogen production, the model computes the temperature variation of the stack, that will be used in the following timestep to estimate the voltage variation. In this step, the geometry of the system is relevant to estimate the temperature variation due to inconstant operation. The geometry of the system affects how heat is distributed and dissipated, which can in turn influence the temperature of the stack.

The electrolyzer stack is fed by a stream of mixture coming from a gas-liquid separator that, according to the manufacturer, is the primary heat loss source inside the system. This component is modelled as a cylindrical tank, half containing the electrolytic solution of water and KOH and half containing the produced hydrogen.

In common installed configurations, the module is located inside a container, which exchanges heat with the environment. Fig. 3 illustrates a section of the modelled tank. According to the current generation (Q_{gain}) and loss (Q_{lost}) of heat, the electrolyzer temperature variation is computed using Eq. (6), where m_{es} and c_{es} are the mass and the specific heat of the electrolytic solution.

$$\Delta T = \frac{Q_{gain} - Q_{lost}}{m_{es} \cdot c_{es}} \tag{6}$$

Heat is generated in the stack when hydrogen production occurs. To prevent overheating, a cooling loop keeps the maximum temperature of the system equal to the rated value of 71 °C. Electrolysis takes place at a voltage higher than the thermoneutral one to overcome losses given by inefficiency of electrochemical reactions and by the electrical and ionic resistance of the cell [27].

The thermoneutral voltage for liquid water electrolysis is denoted as V_{tn} and has a value of 1.48 V [28]. In this condition, the reaction becomes exothermic, and the extra power is dissipated in form of heat. When the amount of hydrogen that the stack is producing in each time instant is known, the function f_{H2-i} extrapolates the corresponding current density that is flowing through the cell, and the function f_{i-v} computes the corresponding voltage.

The difference between the operating voltage and the thermoneutral one, multiplied by the current of the stack, is equal to the generated thermal power (Eq. (7)).

$$q_{gain} = n_{cells} \cdot (V_{op} - V_{tn}) \cdot I \tag{7}$$

During operation, the gas-liquid separator is the main source of thermal losses towards the surrounding environment. Heat is transmitted across a series of resistances: internal convection inside the tank, conduction of tank itself, convection with the air between the tank and the external container, container conduction and eventually external air convection. Lost thermal power is computed according to Eq. (8). Table 1 summarizes meaningful properties of the component geometry for the calculation of the temperature variation.

[1] McPhy Energy, pers. comm.

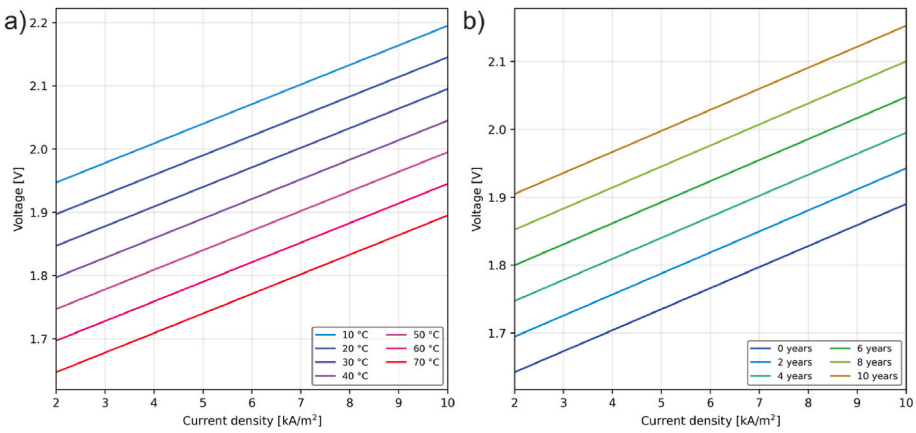

Fig. 2. a) Effect of temperature on the modelled polarization curve for a brand-new electrolyzer cell b) Effect of working time on the modelled polarization curve at rated working temperature (71 °C).

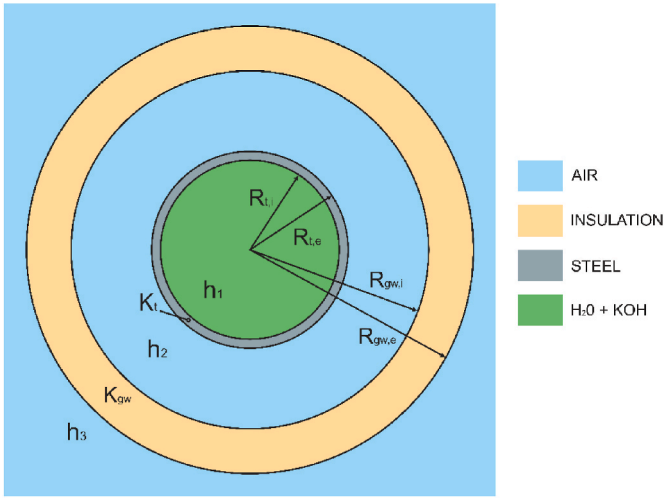

Fig. 3. Scheme of a section of the gas-liquid separator for heat exchange with the external environment.

Table 1
Main characteristics and thermal parameters of different layers of the gas-liquid separator.

Component	material	dimension	coefficient
Gas-liquid separator	$H_2O + KOH$	$R_{t,i} = 30$ cm	$h_1 = 100$ W/m^{2}K
Tank	steel	$R_{t,i} - R_{t,e} = 5$ mm	$k_t = 52$ W/mK
Gap	air	$R_{gw,i} = 1$ m	$h_2 = 10$ W/m^{2}K
Insulation	glass wool	$R_{gw,i} - R_{gw,e} = 5$ mm	$k_{gw} = 0.05$ W/mK
External air	air	–	$h_3 = 20$ W/m^{2}K

$$q_{lost} = \frac{(T_{int} - T_{ext}) \cdot 2\pi L}{\frac{1}{h_1 \cdot R_{t,i}} + \frac{\ln\left(\frac{R_{t,e}}{R_{t,i}}\right)}{k_t} + \frac{1}{h_2 \cdot R_{gw,i}} + \frac{\ln\left(\frac{R_{gw,e}}{R_{gw,i}}\right)}{k_{gw}} + \frac{1}{h_3 \cdot R_{gw,e}}} \quad (8)$$

2.3. Battery energy storage system (BESS)

While the focus of the study is on the electrolyzer, a battery model was considered important for an exhaustive feasibility study. As pointed out in Ref. [29], a storage system may in fact increase the exploitation of the fluctuation caused by the intermittent nature of wind power. According to the manufacturer, electrolyzer modules requires at least 20% of their rated power to start the conversion reaction. The battery can be then a way to extend the working hours of the electrolyzers stack. Lithium-ion batteries have been chosen among the available electrochemical storage systems because of their high efficiency and resilience to cyclic operations [30].

2.3.1. BESS model

The battery model is based on a previous study by some of the authors [31] and the dynamic behavior of the battery has been neglected since its response time is in the order of milliseconds, thus much shorter than the time step considered in the study (10 min). At each time step, the model determines the state of charge (SOC) and the state of health (SOH) of the battery, considering technical limitations. A control system ensures that SOC is allowed to vary in a range between 15% and 95%, considering that full charge-discharge cycles are very harmful in terms of battery degradation.

SOH provides an indication of the aging of a battery compared to ideal conditions; it is expressed as a percentage, where 100% corresponds to new battery conditions. The variation in SOH can be used to estimate how much the battery has aged compared to its ideal conditions. A lower threshold for the SOH can be used as an indicator for the battery replacement, in this study it is considered to be 70% [32].

Another parameter that was considered in the battery model is the C-rate: a measure of the rate at which a battery is charged or discharged in relation to its maximum capacity. A value of 1C means that the battery can be completely charged in 1 h, 2C means that it can be charged in 30 min. This parameter must be limited to avoid abnormal temperature, and consequent efficiency losses and shorter lifetime. In this study, conservative limits of 1C for charge and 2C for discharge have been imposed [33].

2.3.2. BESS control

The battery is employed to support the islanded operation of the system. For its management, a battery control algorithm is applied to the input wind power (P_{wind}) that is produced by the farm. At each timestep, a goal power (P_{goal}) is set. When the input wind power is below the minimum required value by the electrolyzer to work, the goal is to ensure that the module avoids the stand-by mode: at least 20% of the electrolyzer rated power must be provided. When the input power is higher, the goal is to support the electrolyzer operation at rated conditions. The SOC of the battery is updated considering SOH and C-rate limitations.

The control algorithm (similar to that already presented in Ref. [10]) distinguishes two cases: excess power, when the battery must be charged, and required power, when the battery must be discharged. The charging and discharging efficiencies dependency on SOC [34] is considered as shown in Fig. 4. Each time-step, new values for the SOC and the C-rate are computed according to the goal power. Then,

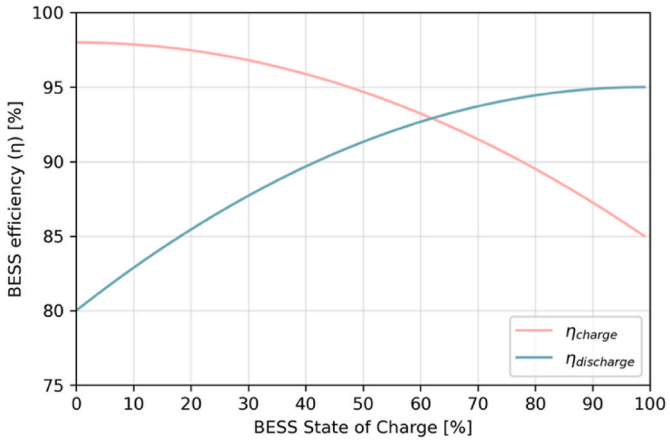

Fig. 4. BESS charging efficiency η_c and discharging efficiency η_d.

considering technical limitations imposed to the two parameters, the power that is actually feasible to send to the electrolyzer from the battery ($P_{to\_electrolyzer}$) is computed. Eventually, the actual SOC that the battery reach at the end of the timestep is obtained.

2.3.3. BESS degradation

The SOH of the battery declines with the charge-discharge cycles that the battery performs (Fig. 5). Each day of operation (d), the SOH of the battery is updated according to Eq. (9). The employed battery degradation model is based on concepts related to material fatigue. The equivalent number of full charge-discharge cycles (EFC) performed by the battery is obtained by means of a Rainflow counting method, as explained in Ref. [35]. The ratio between the latter value and the maximum number of full cycles that the battery can withstand corresponds to the daily degradation of the battery.

$$D_{day} = D_{day-1} + \frac{EFC_{day}}{5200 \cdot (\Delta soc)_{day}^{-1.5}} \tag{9}$$

2.4. Techno-economic quantities

This subsection introduces the main techno-economic parameters utilized to compare performance of different configurations, i.e., the Capacity Factor (CF) and the Levelized Cost Of Hydrogen (LCOH).

2.4.1. Capacity factor (CF)

A first significant technical parameter to assess the performance of a system configuration (composed by the wind farm, the battery energy storage and the electrolyzer stack) is the capacity factor (CF), i.e., the ratio between the actual hydrogen production M_{H_2} and the maximum production that the system would be able to produce in the same time window.

CF indicates how much the installed electrolyzers stack was exploited in a year of operation with respect to one year of operation at rated conditions (Eq. (10)).

$$CF = \frac{M_{H_2}}{P_{el} \cdot \varphi_{id} \cdot \rho_{H_2} \cdot time} \tag{10}$$

2.4.2. Levelized cost of hydrogen (LCOH)

In line with other studies (e.g., Ref. [12]), the LCOH calculation is introduced to estimate which is the optimal combination of battery energy system and electrolyzer stack to be installed in economic terms.

LCOH quantifies how much 1 kg of hydrogen produced by a given configuration costs and it is defined as the ratio between the total expenditure (CAPEX + OPEX) and the total hydrogen production in kilograms (M_{H_2}) [36] (Eq. (11)). Both the numerator and denominator are quantified for each year of operation and actualized to present time. For the analysis, a time frame of 20 years is considered, which corresponds to the expected wind farm lifetime, and a discount rate (r) of 5%.

Other relevant economic parameters (specific costs, scale factors and lifetimes of the main system components) used for the analysis are reported in Table 2.

$$LCOH = \frac{\sum_{t=0}^{T} \frac{CAPEX+OPEX}{(1+r)^t}}{\sum_{t=0}^{T} \frac{M_{H_2}}{(1+r)^t}} \tag{11}$$

Capital expenditures (CAPEX) correspond to the initial investment related to the main components of the system: turbines, electrolyzers and batteries. As shown in Eq. (12), this cost is evaluated starting from a reference cost C_0 that is then scaled to the actual component size x via an economy of scale factor α [42].

$$CAPEX_{component} = C_0 \left(\frac{x}{x_0}\right)^{\alpha} \tag{12}$$

The electrolyzer market is relatively new with respect to the other system components hence its scale factor is considerably lower.

Fig. 6 shows the cost trend of the alkaline electrolyzer when the stack nominal power increases. Orange line shows, as reference, a theoretical linear trend. Blue line shows how the cost scales according to the actual scale function (Eq. (12)), according to the current market scenario. In a future scenario, when the electrolyzer market has reached maturity, the cost could scale according to the green curve, that considers a scale factor closer to well established technologies as wind turbines or batteries.

The degradation of components (calculated by means of the models described in Section 2) is mostly important for this analysis since it gives information on the potential premature substitution of components. According to the manufacturer, an electrolyzer stack must be replaced after ca. 10 years of operation or when the required cell voltage at rated temperature exceeds 2.3 V. The estimated annual rated voltage increase of a cell is around 26 mV. Since a brand-new cell is characterized by a rated voltage of 1.89 V, it is unlikely that this component must be replaced before the end of its life cycle. The stack replacement cost can be considered as 45% of the initial CAPEX of the module.

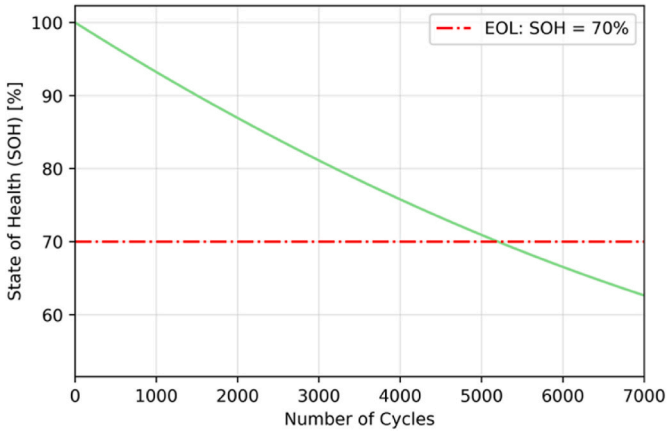

Fig. 5. BESS state of health (SOH) degradation.

Table 2
Main components economic parameters.

Component	Specific cost (C_0)	Scale factor (α)	Lifetime
Turbine	1400 €/kW [37]	0.95	20 years [38]
Electrolyzer	1200 €/kW [39]	0.5[a]	20 years*
BESS	100 €/kWh [40]	0.85	10 years [41]

[a] McPhy Energy, pers. comm.

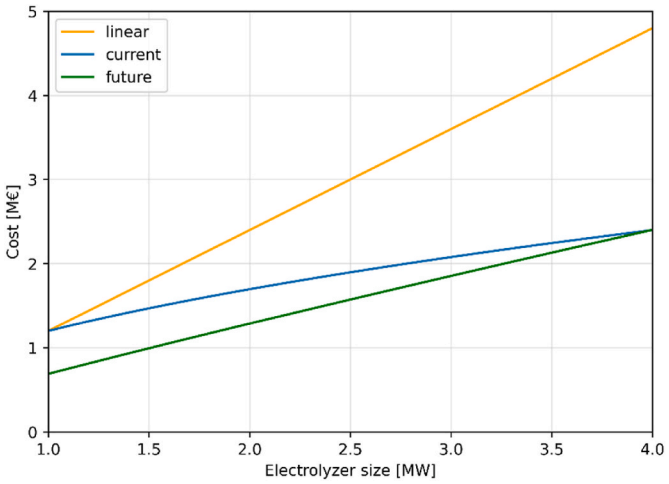

Fig. 6. Electrolyzer cost varying the stack nominal power: linear scaling (orange), current scaling (blue) and future scaling (green).

For what concerns the battery, the estimated drop of state of health in a one-year time frame is around 0.5%, meaning that is unlikely that the battery reaches the 70% lower limit during the component life cycle of 10 years. Results from long-term simulations are shown below to validate this hypothesis.

Operating expenditures (OPEX) correspond to the operation and maintenance cost. As found in several other studies, it can be supposed that the annual OPEX of one component corresponds to a fraction of its CAPEX. For the turbine [43], the electrolyzer [39] and the battery [44], this percentage corresponds to 2% for the initial investment cost.

3. Results

This section presents the main results obtained with the developed simulation framework about the most suitable sizing of electrolyzer modules in combination with the wind farm.

The first subsection "Year-long simulation" describes the results coming from a single combination of a defined number and size of installed electrolyzer modules and battery capacity.

The second subsection, "Battery long-term degradation" shows how much the BESS ages during a whole year of operation.

The third subsection "Techno-economic quantities" presents a sensitivity analysis, related to a preliminary sizing phase, aimed to assess which combinations of above-mentioned quantities are the most effective in techno-economic terms.

3.1. Year-long simulation

The described simulation framework was used to simulate the production of green hydrogen from the wind farm in a one-year time window. A step-by-step simulation keeps track of useful operation quantities such as the temperature of modules, the operating voltage of cells, the resulting conversion factor and the state of health of batteries. The evolution in time of such quantities allows to analyze in detail the transient behavior of the system under variable working conditions.

Fig. 7 (a) shows the variation of previously mentioned quantities for a configuration that combines five electrolyzer modules with a nominal power of 1 MW with a 15 MWh battery. In particular, the figure analyzes the effect of the cool down of modules in non-working hours: when the electrolyzers stack does not receive an input power, the temperature of modules decreases from the operational temperature of 71 °C to lower values.

In Fig. 7 (b), the corresponding cells voltage variation across the year is analyzed. The effect of time degradation of cell voltage is visible as a linearly increasing trend with time. In addition, thermal degradation is visible in the form of spikes that rise the operating cell voltage when modules cool down. In turn, an increase in voltage affects the conversion factor of each module. A higher required voltage means that the cell must absorb more power to work at the same current density.

The conversion factor drop decreases the maximum amount of hydrogen that the cell is able to produce if the available power from the wind farm is lower or equal to the rated power of the module. This effect can be visualized in Fig. 7 (c), where a decreasing linear trend is apparent due to the voltage degradation in time and downward spikes due to the cooling effect of modules.

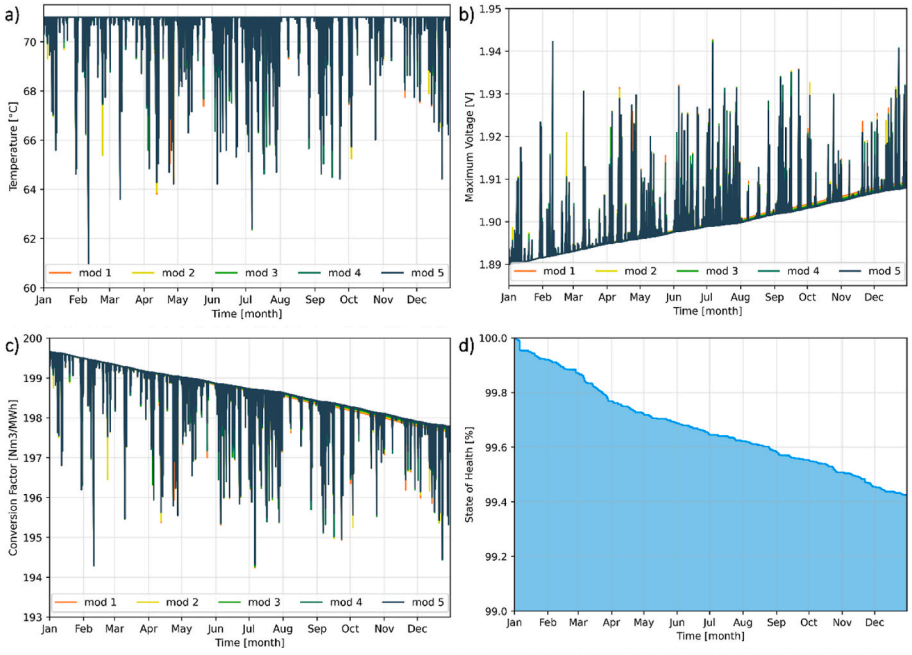

Fig. 7. a) Modules temperature variation; b) Cell voltage variation in modules; c) Modules conversion factor (φ) variation; d) Battery state of health (SOH) degradation.

Concerning the battery SOH, Fig. 7 (d) shows its decrease in time due to the charge and discharge cycles that the battery performs. This analysis allows in fact to evaluate the component degradation across one year of operation; results are then particularly useful for the economic analysis discussed in the following sections.

3.2. Battery long-term degradation

As pointed out before, the state of health of the lithium-ion battery must remain above 70% to prevent a premature substitution of the component. To estimate the maximum degradation that may occur, systems involving different storage sizes and different electrolyzer power levels to be satisfied were simulated across ten years of operation, after which the battery must be substituted anyway.

Fig. 8 (a) shows the SOH trend in time for configurations supported by battery sizes ranging from 1 to 30 MWh. The degradation is higher when the storage size is small because of the widest cycle amplitude that a limited capacity BESS must face when supporting the same utility.

Fig. 8 (b) shows the degradation of a 1 MW battery when supporting electrolyzer power levels ranging from 1 to 14 MW. In this case, a small electrolyzer cannot absorb power production peaks from the WF, entrusting the task entirely to the battery.

Overall, the configuration that showed the highest degradation was the one in which the smallest battery size supported the smallest electrolyzer. That battery arrived to 85% of its health level after 10 years of operation, hence no premature substitution of the component was considered in the techno-economic assessment.

3.3. Techno-economic analysis

The main techno-economic outcomes of the study are reported in this section.

Several configurations of electrolyzers sizes and battery capacities have been tested to assess the optimal combination in techno-economic terms. The considered range for each variable is reported in Table 3. Differently from many studies made so far, real commercial module sizes were considered in the size optimization phase (thus, not varying as a continuous variable). Module of 1, 2 and 4 MW, respectively, were considered. A combination of those sizes was considered to exploit the power production level of the wind farm.

3.3.1. Capacity factor (CF)

The computation of the CF gives an idea on the degree of exploitation of the electrolyzer with respect to a standard scenario of constant operation at rated power. Fig. 9 shows that CF decreases with the installed electrolyzer power and increases with the battery capacity.

Table 3
Range for optimized parameters.

Parameter	Range
Electrolyzer module	1, 2, 4 MW
Electrolyzer power	1–16 MW
BESS capacity	0-30 MWh

Moreover, it can be noticed that the adoption of an energy storage system between the renewable power generation and the electrolyzer module indeed allows to increase the resource exploitation.

Thanks to the employed battery control, the energy storage system extends the working hours of the electrolyzer stack: the power surplus produced by the wind farm is stored in the BESS and redistributed within the time frames of low power generation. In those moments, the minimum required amount of power can be supplied by the BESS even when the wind farm is not producing.

On the other hand, CF inevitably decreases at high installed electrolyzer power levels, since one must bear in mind that the farm often operates below rated. Upon comparison of Fig. 9 (sub-plots (a), (b) and (c)), which compares the results with different electrolyzer sizes, it is apparent that configurations that involve smaller modules can provide a capacity factor slightly higher.

At low installed electrolyzer powers (4 MW) and high battery capacities (30 MWh), a combination of four 1 MW modules reaches a CF near to 64%, while a single 4 MW module reaches lower values (~62%). On average, when comparing configurations with the same power level and battery capacity, 4 MW modules configurations have a capacity factor 2% lower with respect to a combination of 1 MW modules.

Due to the lower power required to start the conversion reaction, configurations that involve smaller modules can reach higher capacity factors for the same total installed electrolyzer power and battery capacity.

Fig. 10 shows the hydrogen production trend of three system configurations during a typical day of low power production. To have an unbiased interpretation of the results, all three configurations are characterized by the absence of BESS and a total installed electrolyzer power of 4 MW.

The first configuration employs four 1 MW modules, the second two 2 MW modules and the third a single 4 MW module. When the power production is above 800 kW, all three configurations produce the same amount of hydrogen (green area), but when the power level drops below this limit, only the first two configurations can operate (orange area). Below 400 kW, only the last configuration continues producing hydrogen (blue area). A more frequent activation during the periods of low power production allows the configuration that involves smaller modules to higher capacity factors.

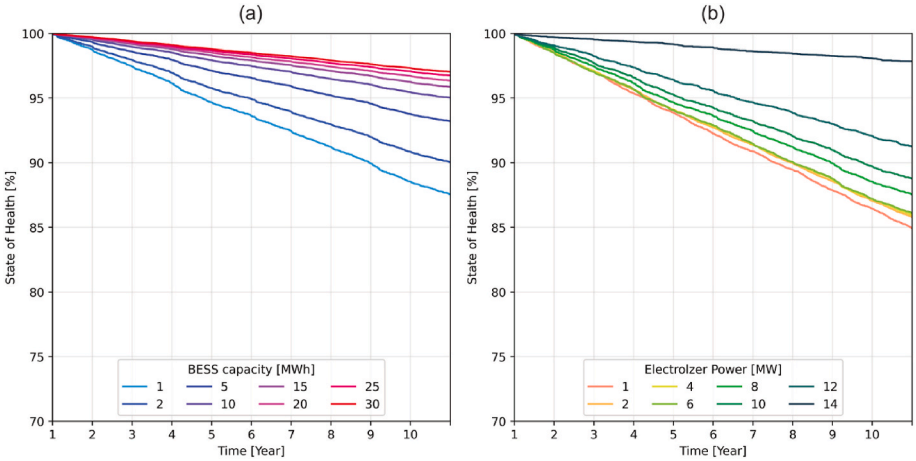

Fig. 8. Battery degradation on 10 years of operation varying a) battery size and b) electrolyzer power to support.

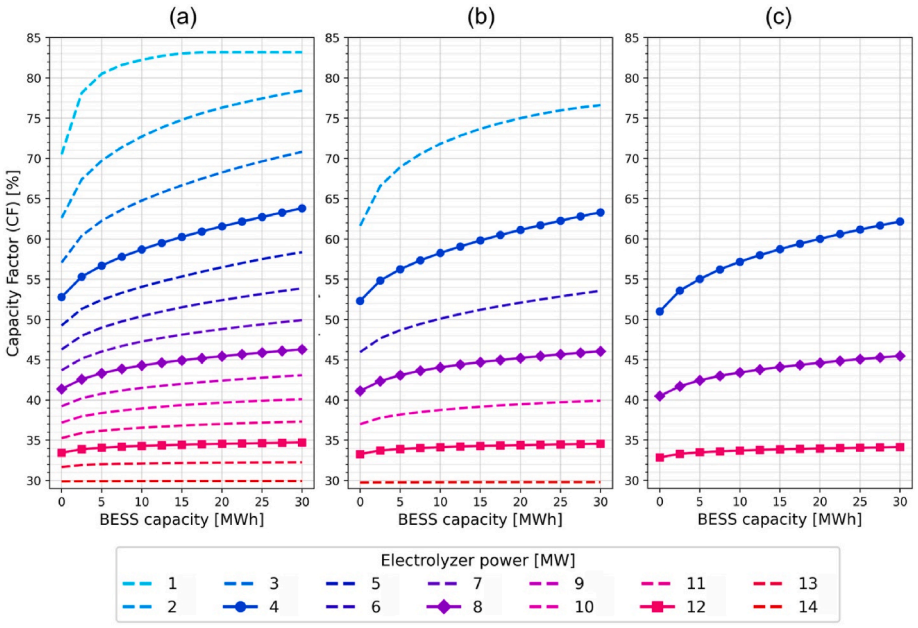

Fig. 9. Capacity Factor (CF) curves comparison among different module size combinations: a) 1 MW modules combinations; b) 2 MW modules combinations; c) 4 MW modules combinations.

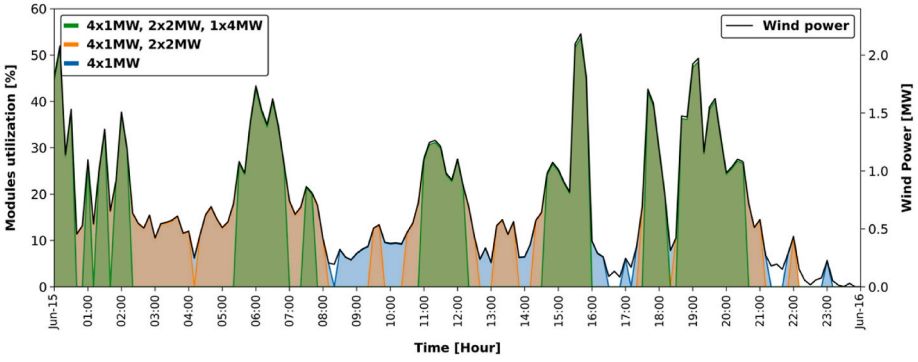

Fig. 10. Hydrogen production by different configurations during a typical operation day.

3.3.2. *Levelized cost of hydrogen (LCOH)*

The LCOH is key to assessing the market potential of the proposed technology and to identify the best combination of components in economic terms.

Fig. 11, which report the resulting LCOH when using electrolyzer modules of 1 MW (a), 2 MW (b) and 4 MW (c), indicate that the

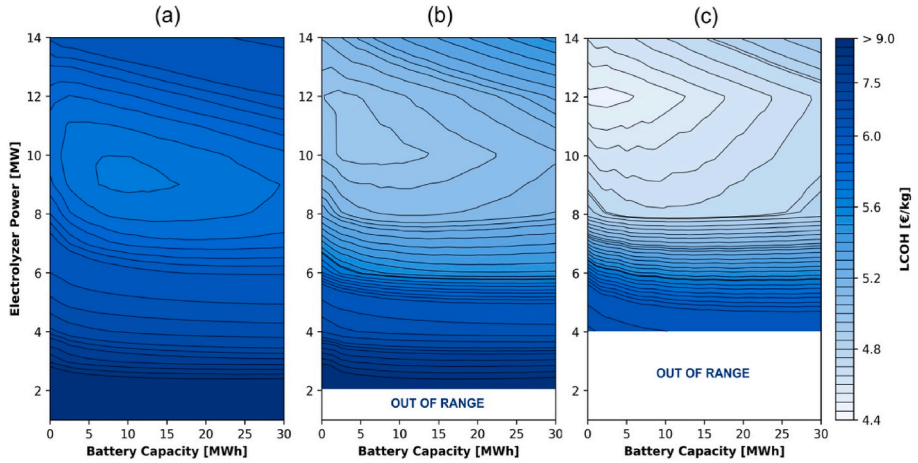

Fig. 11. LCOH zones comparison among different modules combinations: a) 1 MW modules combinations; b) 2 MW modules combinations; c) 4 MW modules combinations.

economic optimum does not necessarily match high-capacity factors. According to the analysis, in configurations that combine 1 MW modules, the LCOH can be lowered down to 5.66 €/kg.

Fig. 11 (a) shows that the most convenient combinations of this module size are given by an installed electrolyzer power between 9 and 10 MW and a large battery capacity between 7.5 and 12.5 MWh, which reaches capacity factors up to 42%. In combinations of this module size, an increase in the battery capacity generally produces a decline in the LCOH: the installation cost increase is in fact not completely balanced by an increment in the amount of hydrogen that can be generated.

Those effects have the same magnitude around the most convenient electrolyzer power levels, and this is reflected by the flat zone that indicates the most convenient combinations. By using 2 MW modules combinations, it is possible to reach a lower LCOH, down to 4.98 €/kg. In this case, the optimal electrolyzer power is slightly higher than before, and around 10–12 MW.

The optimal battery capacity is instead lower, ranging between 5 and 7.5 MWh (Fig. 11 (b)). Due to the higher installed power and lower battery capacities, the capacity factors that characterize those configurations are in the order of 38%.

The lowest value of LCOH can be reached by 4 MW modules combinations, down to 4.48 €/kg. In this case, the optimal installed size is 12 MW, and the cost-effectiveness of a BESS becomes less evident (Fig. 11 (c)). Combinations of this module size that involve small battery capacities between (0–5 MWh) reach lower capacity factors (~33%) but produce the most economically competitive hydrogen.

Results show that configurations that produce the most competitive green hydrogen in terms of LCOH are characterized by big modules combinations and low battery capacities. Thanks to economy of scale, bigger modules are considerably cheaper than smaller ones and make economically convenient to install higher electrolyzer powers. This convenience is not balanced by the lower exploitation of the bigger module that requires a higher minimum power to start the conversion.

Batteries are convenient in small modules configurations, where an energy storage system can rise considerably the capacity factor of the system. In combination with bigger modules, this effect has a lower impact and the initial expenditure for a higher-capacity battery is not recovered by the increment in hydrogen production.

3.4. Multi-size combinations

In this section, the coupling of different sizes of modules was considered to perform a global assessment of the optimal electrolyzer power to install. In this way, it is possible to cover all the electrolyzer power range using combinations of big and small modules and results are not limited by multiplication constraints of a single building block size. Due to the lower operational limit of alkaline electrolyzers and the economy of scale of the component, the coupling of small and big modules also aims to increase the capacity factor of the system while maintaining a lower investment cost.

Several different configurations were simulated, in which combinations of 1, 2 and 4 MW modules were used as building blocks to reach electrolyzer power levels ranging from 1 to 14 MW, supported by battery capacities from 0 to 30 MWh.

Fig. 12 (a) shows the global LCOH colormaps for the current market scenario, characterized by very low capex scale factor for the electrolyzer of 0.5. The multi-size analysis confirmed results from the single-size optimization: the lowest LCOH is reached by a combination of 3 modules of 4 MW coupled with batteries from 0 to 5 MWh. The global minimum for the LCOH is still 4.48 €/kg.

Results show that is still not convenient to invest in small scale electrolyzers. Currently, the considerably higher cost of small modules makes their installation still questionable for an economic point of view, even if they may rise the capacity factor of the system.

Instead, Fig. 12 (b) considers a possible future market scenario, in which the electrolyzer technology has reached maturity. In this context, it was assumed a specific cost of 600 €/kW for the component and a capex scale factor of 0.9, in line to the current scale for batteries and wind turbines. Here the optimization reaches an optimal electrolyzer power to install of 13 MW, pairing 3 modules of 4 MW with a 1 MW module.

Results show that, with an increase of electrolyzer size, the optimal battery capacity range decreases and lies in the range between 0 and 2.5 MWh. This configuration reaches a LCOH of 4.24 €/kg, even if the higher installed power makes the CF decrease to 31.9%.

4. Conclusions

The development of a reliable simulation framework for techno-economic analyses on alkaline electrolyzers is key to estimating the real capabilities of a hydrogen production system fed by intermittent renewables. The numerical models developed in this study allow to consider this aspect in the context of a techno-economic analysis.

The proposed step-by-step simulation also allows to check the effect of system modifications on the main quantities that affect the electrolysis process as the modules temperature and voltage and their implication for the total hydrogen producibility. Therefore, this framework also allows testing different control methods for the hydrogen production system so as to increase synergy between renewable generators, batteries and electrolyzers.

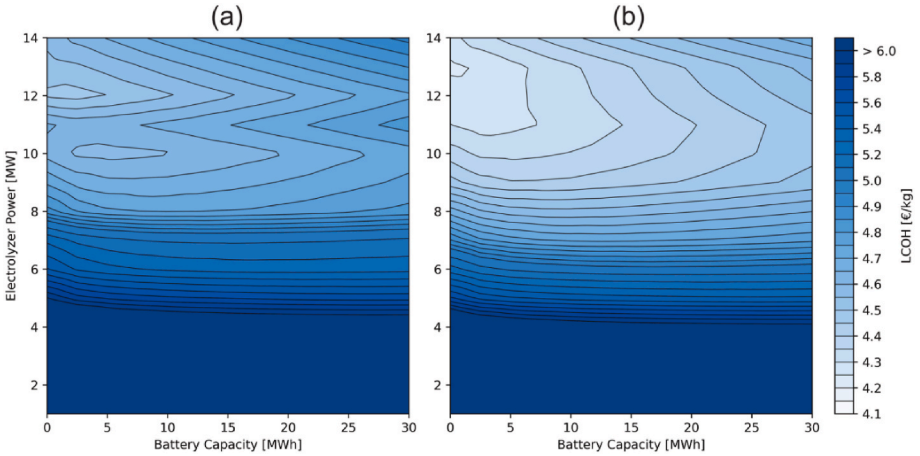

Fig. 12. LCOH results for multi-size modules combinations varying electrolyzer power and battery capacity. Comparison between the actual and future market scenario for electrolyzers: a) electrolyzer cost: 1200 €/kW and scale factor of 0.5; b) electrolyzer cost: 600 €/kW and scale factor of 0.9.

4.1. Main outcomes

The two presented techno-economic parameters, capacity factor (CF) and levelized cost of hydrogen (LCOH), proved to be useful not only to estimate a certain configuration performance among a defined time frame, but also as a fundamental tool to compare different possible configurations. In this analysis, the capacity factor allowed to understand the impact of the inclusion of an energy storage system and the benefit of a module that requires less power to start the production process, two effects that are crucial when the primary energy source is intermittent. The main outcomes of the work are summarized below.

- Results show that a high-capacity battery can increase the CF by up to +10%, thus leading to a higher exploitation of the electrolyzers stack and an increment in the produced hydrogen.
- In addition to the capacity factor, the LCOH was proved to be a crucial parameter in the sizing phase: due to the economy of scale, results show that is convenient to install high-power modules even if their degree of exploitation remains lower with respect to smaller power modules.
- The battery was proved to increase the exploitation of the renewable power source, but its benefit becomes less apparent when the installed electrolyzer power rises. For this reason, the most convenient configurations that involve high-power modules do not include a high-capacity battery.
- Eventually, according to the results obtained, most convenient configurations result in a LCOH in the order of 4.48 €/kg, i.e., close to what is reported in literature for wind powered water electrolysis [10].
- The multi-size simulation confirmed that the previous single-size combination leads to the best economic outcome even when compared to combinations of different module sizes.
- The future success of green hydrogen will be determined by the technological development of electrolyzers.

4.2. Impact and future developments

Together with other renewable sources, wind power has the potential of contributing massively to the decarbonization of the energy production sector. However, the inherent variability of renewable energy production stresses the importance of developing advanced and cheap storage systems and alternative energy vectors. This is necessary to increase the flexibility of renewable energy-based power systems and effectively spread their use. Green hydrogen represents a suitable candidate for both storage and energy transmission and could help the energy transition in many sectors.

The adoption and spread of alkaline electrolyzers technology, along with the resulting cost reduction due to economy of scale, could be the key to ensuring the success of green hydrogen. A low LCOH translates in a lower storage cost in scenarios that consider the power-to-gas technology as a suitable seasonal storage mean, or lower manufacturing expenses when green fuels are expected to replace fossils in carbon intensive processes.

The results of the present analysis show that, given current prices, today is still more convenient to invest in big electrolyzers modules that show a lower specific cost, even if their source exploitation is lower.

A cost reduction for small scale electrolyzer modules, that have been shown to have higher capacity factors when coupled with intermittent sources, would result in cheap but high-performance hydrogen production systems, leading to a certain drop in the resulting LCOH.

Results of the analysis show that small scale electrolyzers, if competitively priced, are key to harnessing the power fluctuations of renewables, especially when connected to remote locations with a limited connection to the electrical grid. In a future market situation in which the electrolyzer technology has reached maturity, the price of hydrogen produced by an optimized configuration can be reduced to 4.24 €/kg.

To move towards energy systems with high shares of renewable energy supported by storage means as green hydrogen, there is a need for policy support and investment in research and development of electrolysis technology. This will help the cost reduction of hydrogen and make it more competitive with respect to traditional fossil fuels. Further research in alkaline electrolyzer technology may help to disclose the full potential of power-to-gas and pave the way for its widespread diffusion.

CRediT authorship contribution statement

Francesco Superchi: Conceptualization, Methodology, Software, Validation, Formal analysis, Investigation, Data curation, Writing – original draft, Visualization. **Francesco Papi:** Methodology, Writing – review & editing. **Andrea Mannelli:** Methodology, Software. **Francesco Balduzzi:** Conceptualization, Methodology. **Alessandro Bianchini:** Conceptualization, Methodology, Investigation, Resources, Data curation, Writing – review & editing, Supervision, Project administration, Funding acquisition. **Francesco Maria Ferro:** Conceptualization, Methodology.

Declaration of competing interest

The authors declare that they have no known competing financial interests or personal relationships that could have appeared to influence the work reported in this paper.

Data availability

Data will be made available on request.

Acknowledgments

A first version of this study was presented at the 17th SDEWES Conference, which was held in Paphos (Cyprus) on November 6–10, 2022. Authors would like to acknowledge the conference organizers for the opportunity to present and discuss this work outcomes with a unique group of experts and researchers.

References

[1] A. Ajanovic, M. Sayer, R. Haas, The economics and the environmental benignity of different colors of hydrogen, Int. J. Hydrogen Energy (2022), https://doi.org/10.1016/j.ijhydene.2022.02.094.
[2] M. Götz, J. Lefebvre, F. Mörs, A. McDaniel Koch, F. Graf, S. Bajohr, et al., Renewable Power-to-Gas: a technological and economic review, Renew. Energy 85 (2016) 1371–1390, https://doi.org/10.1016/j.renene.2015.07.066.
[3] E. Rusu, F. Onea, A parallel evaluation of the wind and wave energy resources along the Latin American and European coastal environments, Renew. Energy 143 (2019) 1594–1607, https://doi.org/10.1016/j.renene.2019.05.117.
[4] M.M. Nezhad, M. Neshat, D. Groppi, P. Marzialetti, A. Heydari, G. Sylaios, et al., A primary offshore wind farm site assessment using reanalysis data: a case study for Samothraki island, Renew. Energy 172 (2021) 667–679, https://doi.org/10.1016/j.renene.2021.03.045.
[5] P. Denholm, T. Mai, Timescales of energy storage needed for reducing renewable energy curtailment, Renew. Energy 130 (2019) 388–399, https://doi.org/10.1016/j.renene.2018.06.079.
[6] H. Lin, Q. Wu, X. Chen, X. Yang, X. Guo, J. Lv, et al., Economic and technological feasibility of using power-to-hydrogen technology under higher wind penetration in China, Renew. Energy 173 (2021) 569–580, https://doi.org/10.1016/j.renene.2021.04.015.
[7] G. Salgi, B. Donslund, P. Alberg Østergaard, Energy system analysis of utilizing hydrogen as an energy carrier for wind power in the transportation sector in Western Denmark, Util. Pol. (2008), https://doi.org/10.1016/j.jup.2007.11.004.
[8] Z. Fan, E. Ochu, S. Braverman, Y. Lou, G. Smith, A. Bhardwaj, et al., Green Hydrogen in a Circular Carbon Economy: Opportunities and Limits, COLUMBIA SIPA, 2021.
[9] F. Superchi, A. Mati, M. Pasqui, C. Carcasci, A. Bianchini, Techno-economic study on green hydrogen production and use in hard-to-abate industrial sectors, J. Phys. Conf. Ser. 2385 (2022), 012054, https://doi.org/10.1088/1742-6596/2385/1/012054.

[10] J.-L. Fan, P. Yu, K. Li, M. Xu, X. Zhang, A levelized cost of hydrogen (LCOH) comparison of coal-to-hydrogen with CCS and water electrolysis powered by renewable energy in China, Energy (2022), https://doi.org/10.1016/j.energy.2021.123003.
[11] D. Mazzeo, M.S. Herdem, N. Matera, J.Z. Wen, Green hydrogen production: analysis for different single or combined large-scale photovoltaic and wind renewable systems, Renew. Energy 200 (2022) 360–378, https://doi.org/10.1016/j.renene.2022.09.057.
[12] R. Bhandari, R.R. Shah, Hydrogen as energy carrier: techno-economic assessment of decentralized hydrogen production in Germany, Renew. Energy (2021), https://doi.org/10.1016/j.renene.2021.05.149.
[13] B. Nastasi, S. Mazzoni, D. Groppi, A. Romagnoli, D. Astiaso Garcia, Optimized integration of Hydrogen technologies in Island energy systems, Renew. Energy 174 (2021) 850–864, https://doi.org/10.1016/j.renene.2021.04.137.
[14] M. Genovese, P. Fragiacomo, Parametric technical-economic investigation of a pressurized hydrogen electrolyzer unit coupled with a storage compression system, Renew. Energy 180 (2021) 502–515, https://doi.org/10.1016/j.renene.2021.08.110.
[15] M. Rezaei, N. Naghdi-Khozani, N. Jafari, Wind energy utilization for hydrogen production in an underdeveloped country: an economic investigation, Renew. Energy 147 (2020) 1044–1057, https://doi.org/10.1016/j.renene.2019.09.079.
[16] C. Marino, A. Nucara, M.F. Panzera, M. Pietrafesa, V. Varano, Energetic and economic analysis of a stand alone photovoltaic system with hydrogen storage, Renew. Energy 142 (2019) 316–329, https://doi.org/10.1016/j.renene.2019.04.079.
[17] D. Chade, T. Miklis, D. Dvorak, Feasibility study of wind-to-hydrogen system for Arctic remote locations – grimsey island case study, Renew. Energy 76 (2015) 204–211, https://doi.org/10.1016/j.renene.2014.11.023.
[18] J. Brauns, T. Turek, Alkaline water electrolysis powered by renewable energy: a review, Processes 8 (2020) 248, https://doi.org/10.3390/pr8020248.
[19] Z. Wang, X. Zhang, A. Rezazadeh, Hydrogen fuel and electricity generation from a new hybrid energy system based on wind and solar energies and alkaline fuel cell, Energy Rep. 7 (2021) 2594–2604, https://doi.org/10.1016/j.egyr.2021.04.060.
[20] A. Khalilnejad, G.H. Riahy, A hybrid wind-PV system performance investigation for the purpose of maximum hydrogen production and storage using advanced alkaline electrolyzer, Energy Convers. Manag. 80 (2014) 398–406, https://doi.org/10.1016/j.enconman.2014.01.040.
[21] R. Ahshan, A. Onen, A.H. Al-Badi, Assessment of wind-to-hydrogen (Wind-H2) generation prospects in the Sultanate of Oman, Renew. Energy 200 (2022) 271–282, https://doi.org/10.1016/j.renene.2022.09.116.
[22] Y. Anouti, R. Kombargi, S. Elborai, R. Hage, The Dawn of Green Hydrogen: Maintaining the GCC's Edge in a Decarbonized World, Strategy&, 2020.
[23] M. Bodner, A. Hofer, V. Hacker, H2 generation from alkaline electrolyzer, WIREs Energy Environ. (2015), https://doi.org/10.1002/wene.150.
[24] Ø. Ulleberg, Modeling of advanced alkaline electrolyzers: a system simulation approach, Int. J. Hydrogen Energy (2003), https://doi.org/10.1016/S0360-3199(02)00033-2.
[25] E. Amores, J. Rodríguez, J. Oviedo, A. Lucas-Consuegra, Development of an operation strategy for hydrogen production using solar PV energy based on fluid dynamic aspects, Open Eng. (2017), https://doi.org/10.1515/eng-2017-0020.
[26] Z. Ren, J. Wang, Z. Yu, C. Zhang, S. Gao, P. Wang, Experimental studies and modeling of a 250-kW alkaline water electrolyzer for hydrogen production, J. Power Sources 544 (2022), 231886, https://doi.org/10.1016/j.jpowsour.2022.231886.
[27] G. Tsotridis, A. Pilenga, EU Harmonised Protocols for Testing of Low Temperature Water Electrolysers, Publications Office of the European Union, 2021, https://doi.org/10.2760/58880.
[28] E. Zoulias, E. Varkaraki, N. Lymberopoulos, C. Christodoulou, G. Karagiorgis, A review on water electrolysis, Crprus J. Sci. Technol,4, (2004) 41–71.
[29] D. Ipsakis, S. Voutetakis, P. Seferlis, F. Stergiopoulos, C. Elmasides, Power management strategies for a stand-alone power system using renewable energy sources and hydrogen storage, Int. J. Hydrogen Energy (2009), https://doi.org/10.1016/j.ijhydene.2008.06.051.
[30] K.C. Divya, J. Østergaard, Battery energy storage technology for power systems—an overview, Elec. Power Syst. Res. (2009), https://doi.org/10.1016/j.epsr.2008.09.017.
[31] A. Mannelli, F. Papi, G. Pechlivanoglou, G. Ferrara, A. Bianchini, Discrete wavelet transform for the real-time smoothing of wind turbine power using Li-ion batteries, Energies (2021), https://doi.org/10.3390/en14082184.
[32] L. Canals Casals, M. Rodríguez, C. Corchero, R.E. Carrillo, Evaluation of the End-Of-Life of Electric Vehicle Batteries According to the State-Of-Health, World Electr Veh J, 2019, https://doi.org/10.3390/wevj10040063.
[33] MIT Electric Vehicle Team, A Guide to Understanding Battery Specifications, 2008.
[34] L. Pugi, Meccatronica. Elementi di Trazione Elettrica, 2017.
[35] Y. Shi, B. Xu, Y. Tan, D. Kirschen, B. Zhang, Optimal battery control under cycle aging mechanisms in pay for performance settings, IEEE Trans. Automat. Control (2019), https://doi.org/10.1109/TAC.2018.2867507.
[36] C. Wulf, P. Zapp, Assessment of system variations for hydrogen transport by liquid organic hydrogen carriers, Int. J. Hydrogen Energy (2018), https://doi.org/10.1016/j.ijhydene.2018.01.198.
[37] T. Stehly, P. Beiter, P. Duffy, 2019 Cost of Wind Energy Review, National Renewable Energy Laboratory, 2020.
[38] B. Pakenham, A. Ermakova, A. Mehmanparast, A review of life extension strategies for offshore wind farms using techno-economic assessments, Energies (2021), https://doi.org/10.3390/en14071936.
[39] M. Minutillo, A. Perna, A. Forcina, S. Di Micco, E. Jannelli, Analyzing the levelized cost of hydrogen in refueling stations with on-site hydrogen production via water electrolysis in the Italian scenario, Int. J. Hydrogen Energy (2021), https://doi.org/10.1016/j.ijhydene.2020.11.110.
[40] IRENA, Electricity Storage and Renewables: Costs and Markets to 2030, International Renewable Energy Agency, 2017.
[41] H. Beltran, P. Ayuso, E. Pérez, Lifetime expectancy of Li-ion batteries used for residential solar storage, Energies (2020), https://doi.org/10.3390/en13030568.
[42] K.K. Humphreys, Jelen's Cost and Optimization Engineering, McGraw-Hill, 1991.
[43] K.A. Adeyeye, N. Ijumba, J.S. Colton, A techno-economic model for wind energy costs analysis for low wind speed areas. Processes. https://doi.org/10.3390/pr9081463, 2021.
[44] M. Davison, J. Cranney, T. Summers, C. Townsend, Decentralised Energy Market for Implementation into the Intergrid Concept - Part 2, Integrated System, 2018, pp. 287–293, https://doi.org/10.1109/ICRERA.2018.8566719.